Atmósfera 37, 311-344 (2023)
https://doi.org/10.20937/ATM.53159

Spatiotemporal distributions of ultraviolet radiation from OMI orbital data and relationships with total O_3 and total NO_2

Adriana BECERRA-RONDÓN[1]*, Jorge DUCATI[1] and Rafael HAAG[2]

[1] *Centro Estadual de Pesquisas em Sensoriamento Remoto e Meteorologia, Universidade Federal do Rio Grande do Sul, Av. Bento Gonçalves, 9500, Porto Alegre, RS, Brazil.*
[2] *Universidade Estadual do Rio Grande do Sul, Av. Bento Gonçalves, 8855, Porto Alegre, RS, Brazil.*
*Corresponding author; email: abecerrarondon@gmail.com

Received; December 30, 2021; accepted: June 9, 2022

RESUMEN

La radiación ultravioleta (RUV) desempeña un papel clave en la fotoquímica de la atmósfera a través de procesos de absorción o dispersión por sus componentes (ozono, nubosidad, aerosoles y contaminantes en la troposfera). Cuantificar la RUV de forma espacial y temporal y conocer su relación con las variables moduladoras es importante para el estado de Rio Grande do Sul, una región con una de las tasas de neoplasias cutáneas más altas de Brasil. En este estudio se utilizaron los datos de radiación ultravioleta para la región, adquiridos por el Instrumento de Monitoreo de Ozono (OMI, por su sigla en inglés) para el periodo 2006-2020, expresados en términos de dosis diaria eritematosa (DDE), con el objetivo de cuantificar la incidencia de la RUV, su estabilidad en el tiempo y distribución espacial. Nuestros resultados muestran que para esta área de estudio la radiación varía de 3300 a 3700 J m^{-2}, con un gradiente latitudinal de 66.7 J m^{-2} por grado, con máximos registrados en diciembre (6028 J m^{-2}, verano) y mínimos en junio (1123 J m^{-2}, invierno). El 29.76% del área tuvo una tendencia decreciente a largo plazo (valor z = –2), mientras que el 6.19% del área tuvo una tendencia creciente (valor z = 5). Durante el periodo estudiado de 15 años, las ocurrencias de valores altos de DDE se correlacionaron negativamente con el O_3 total como relación dominante, registrándose también correlaciones positivas o negativas con el NO_2 total supeditadas a la época o región investigadas.

ABSTRACT

Ultraviolet radiation (UVR) plays a key role in the photochemistry of the atmosphere, through absorption or dispersion processes by its constituents (ozone, cloudiness, aerosols, and pollutants in the troposphere). Quantifying UVR in a spatial-temporal way and knowing its relationships with modulating variables is important for Rio Grande do Sul State, a region with one of Brazil's highest skin neoplasms rates. Ultraviolet radiation data for the region, acquired by the Ozone Monitoring Instrument (OMI) for the period 2006 to 2020, and expressed in terms of erythemal daily dose (EDD), was used in this study, with the objective of quantifying UVR incidence and its stability in time and spatial distribution. Our results show that for this study area the radiation varies from 3300 to 3700 J m^{-2}, with a latitudinal gradient of 66.7 J m^{-2} per degree, with maxima recorded in December (6028 J m^{-2}, summer) and minima in June (1123 J m^{-2}, winter). A long-term decreasing trend of 29.76% (z value = –2) was observed in the area, while 6.19% of the area had an increasing trend (z value = 5). During the studied period of 15 years, occurrences of high values of EDD were negatively correlated with total O_3 as the dominant relationship. Positive or negative correlations with total NO_2 were also recorded, depending on the investigated season or region.

Keywords: erythemal daily dose, atmospheric constituents, Brazil.

1. Introduction

From the total energy emitted by the Sun, only 8% of what arrives at the top of Earth's atmosphere is ultraviolet radiation, being still reduced to 4% upon arriving at the Earth's surface due to physical processes in the atmosphere and to additional—geographical, temporal, astronomical, and others—factors (Iqbal, 1983; Huffman, 1992; Guarnieri et al., 2004; Silva et al., 2008; Fountoulakis et al., 2020). This radiation falls mainly into the UV-A range (315-400 nm), which has low atmospheric absorption, and in the UV-B range (280-315 nm) which, even if less intense, is important to several photochemical and biological processes. A third component, UV-C (200-280 nm) is absorbed into the stratosphere during the process of ozone layer formation (Koller, 1965; Robinson, 1966; Guarnieri et al., 2004; Sliney, 2007; Bilbao et al., 2011; Andrade and Tiba, 2016). Monitoring of UV intensity and its fluctuation is important for biological and human health issues, and one of the most used quantifying parameters is the erythemal daily dose (EDD) expressed in J m^{-2} and defined as the integration over the day of the incoming ultraviolet irradiance on a horizontal surface weighted with the erythema action spectrum (McKinlay and Diffey, 1987; WMO, 2007).

Since the ozone depletion detection (Farman et al., 1985), efforts have been made to quantify EDD magnitude and to estimate long-term variation trends towards higher values in ultraviolet radiance, being this variation continuously estimated from satellite measurements, with a large spatial cover and with data records sufficient to produce trend estimates (Ialongo et al., 2008; Herman, 2010), mostly focused on specific regions. The factors affecting ultraviolet radiation are generally well known, and the importance of each factor varies with latitude, climate, and the amount of atmospheric pollution at each site, giving origin to non-linear interactions involving complex absorption and scattering processes (Koronakis et al., 2002; Kerr and Fioletov, 2008).

The main parameter modulating ultraviolet absorption is stratospheric ozone (90% of total O_3), which presents a seasonal pattern due to natural processes of formation, transport, and destruction. Ozone concentrations are at their lowest levels in fall and highest in spring (Wakamatsu et al., 1989; André et al., 2003). However, this variability is influenced by natural phenomena and anthropogenic activities (Fahey and Hegglin, 2011; Bais et al., 2015), the latter being linked to the industrial production of nitrogen dioxide (NO_2) formed from the oxidation of nitrous oxide (N_2O) coming from the troposphere. NO_2 can attain high concentrations in the stratosphere (90% of all NO_2), where it destroys O_3 through catalytic processes by sequestering active radicals (Seinfeld and Pandis, 1998).

The impact of ultraviolet solar radiation on environmental and human health is well known by the scientific community (Davis and Sims, 1983; Caldwell et al., 2003; Tiegte et al., 2007; Cardoso, 2011; Rodríguez, 2017). However, the knowledge of variability and quantity of spatiotemporal ultraviolet radiation and its relationship to processes in the atmosphere (ozone formation, ozone hole, etc.) has received considerable attention from research projects (Grant and Heisler, 2000; Alados-Arboledas et al., 2003; Efstathiou et al., 2005; Bais et al., 2007; Kerr and Fioletov, 2008; Meleti et al., 2009; Barnard and Wenny 2010; Elsner et al., 2010; Rieder et al., 2010; Antón et al., 2012; Bernhard et al., 2013; Wolfram et al., 2013; Lopo et al., 2014; Liu et al., 2017; Čížková et al., 2018; Jebar et al., 2019; Becerra-Rondón et al., 2021; Gholamnia et al., 2021; Raptis et al., 2021). In this context, the southern part of South America, being closer to the Antarctic ozone hole, is an area exposed to high levels of ultraviolet radiation throughout the year (Corrêa and Pires 2013; Zaratti et al., 2014), making this region important (Díaz, 2006) at a global scale for UV studies.

While stratospheric ozone is the major atmospheric absorber of ultraviolet radiation, local changes in air pollutants may mask an ultraviolet radiation increase associated with low total ozone episodes, especially in the presence of aerosols (Meleti et al., 2009). This confusing factor may be considered by analyzing the ozone time series, helping to understand UV relationships with pollutants. Besides, considering that for southern Brazil ultraviolet fluxes show significant variability between seasons (Kirchhoff et al., 2000; Guarnieri et al., 2004; Kerr and Fioletov, 2008), quantifying UV variability becomes important on decision-making processes aiming to mitigate effects from exposition to ultraviolet radiation. Based on these perceptions, the objective of this research was: (a) to perform an evaluation, at pixel scale, of

the long-term UV variability in Rio Grande do Sul State; (b) to estimate time trends in this variability, and (c) to investigate possible relationships between UV higher values with total O_3 and total NO_2. To this end, satellite data was our primary source of information. Our research will be presented in the following sections.

2. Material and methods

2.1 Study area

Rio Grande do Sul is the Brazilian southernmost state, having international borders with Argentina to the west and Uruguay to the south (Fig. 1). Its area is 281 707 km², and with more than 11.5 million inhabitants it is the fifth most populated state in the country. The region has a humid subtropical climate with a large seasonal variation with hot summers and well-defined cold winters. Mean temperatures vary from 15 to 18 ºC, with lows as much as –10 ºC (June and July) and highs going up to 40 ºC (December to March) (Livi, 2002). The surface elevation ranges from sea level up to 1200 m with the highest points northeast of the state (Fig. 1).

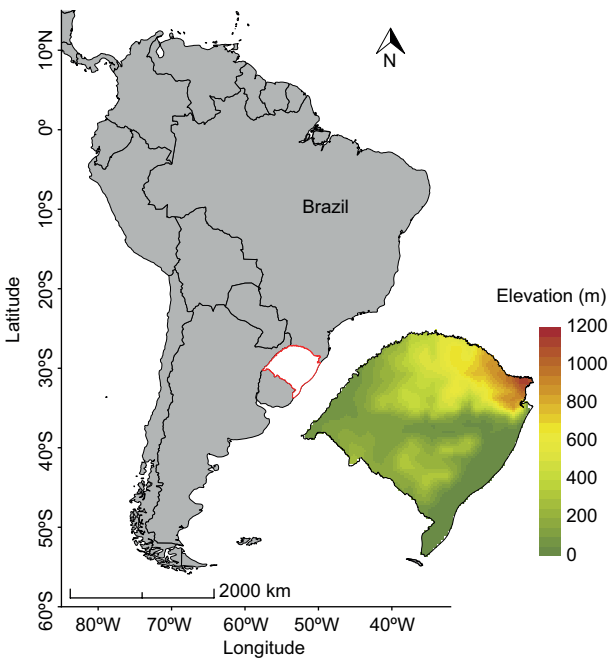

Fig. 1. Location (red contour) and topographic representation (right) of the Rio Grande do Sul State, Brazil.

2.2 Data source

This research was performed from data acquired by the Ozone Monitoring Instrument (OMI) onboard satellite Aura. This sensor is equipped with a spectrometer pointed to the nadir which measures the ultraviolet light (264-504 nm) coming from the Sun and back-scattered by the atmosphere. The differential optical absorption spectroscopy (DOAS) and total ozone mapping spectrometer (TOMS) algorithms were developed to derive several products (Levelt et al., 2006), of which we used nitrogen dioxide (OMNO2d) derived from DOAS and, from TOMS, total ozone (OMTO3d), and EDD (OMUVBd) (Krotkov et al., 2006; Tanskanen et al., 2006). For the product OMNO2d (total column density) data is provided in molecules cm^{-2}, at a spatial resolution of 0.25º × 0.25º (lat/lon), and with a daily frequency. Product OMTO3d (total column density) is also daily but with 1.0º × 1.0º (lat/lon) spatial resolution and in Dobson units (where 1 DU = 2.7×10^{18} molecules O_3 cm^{-2}). Product OMUVBd (cumulative daily dose) is in J m^{-2}.

In this study, information of 15 years (2006-2020) including 5452 images with daily measurements (99% of the series) were used to assess and analyze EDD distributions above the study area. This data was acquired from the data provider GES-DISC (NASA, 2021) and processed using free software RStudio. The spatial resolution of products OMUVBd and OMTO3d was resampled from 1.0º × 1.0º to 0.25º using a RStudio functionality to have uniformity with product OMNO2d. For this 0.25º resolution, the study area is covered by 420 cells.

2.3 Analysis

The spatiotemporal analysis of the long-term (2006-2020) EDD consisted of two parts: (1) variation and trend, and (2) relationships of total O_3 and total NO_2 with higher values of EDD. All the analyses and maps have been processed using statistical functionalities of the software R, version 4.0.5 (R Core Team, 2021). The spatiotemporal variations and the corresponding trends were obtained through the following calculations:

The mean per cell for all 420 cells of the study area for three periods (yearly, monthly and seasonal), using their daily values, was calculated as follows:

$$Var_{i=}\frac{\sum_{t\ enddate}^{startdate} Var_{i,t}}{n} \quad (1)$$

where *Vari* is the mean of the variable in each cell for the respective period; the start and end dates correspond to the first and last date of each period; *n* is the number of days in the period.

The coefficient of variation (CV), which is a statistical measure of the dispersion of data points in a data series around the mean, is expressed as:

$$CV = \frac{\sigma}{\mu} * 100 \quad (2)$$

where σ is the standard deviation and μ is the mean.

From annual means of EDD, the spatiotemporal trend was determined using the Mann-Kendall trend test and Theil-Sen's slope estimator (Mann, 1945; Kendall, 1975), both of them being nonparametric tests. The Mann-Kendall test indicates trend and Theil-Sen's slope estimator indicates the slope of this trend, as follows:

$$Q = \frac{EDD_i - EDD_j}{T_i - T_j} \quad (3)$$

where EDD_i and EDD_j indicate the sequential data values of the time series in the years T_i and T_j, respectively, with $j > i$. The calculated Q is the estimated magnitude of the trend slope in the time series of the data, where negative values indicate a downward trend and positive values indicate an upward trend.

To evaluate the relationships between higher values of EDDs with the variables total O_3 and total NO_2, we compiled the spatial and temporal distribution of EDDs at each month for the period 2006-2020 (Fig. 2a). We were then able to establish the 90th percentile (EDD_{90+}) by pixel in each month (Fig. 2b). Once the EDD_{90+} days were identified and the values of total O_3 and total NO_2 were selected, corresponding to these higher UV values for the concerned pixels, we performed a partial correlation (rpartial) and we valued only those results with a level of statistical significance $\alpha \leq 0.05$. This method allowed us to evaluate the correlation between two variables considering the effect (variance) of a third one (Fig. 2c), and is typically applied when there is reasonable evidence of correlations between the considered variables, which is the case involving UV, NO_2, and O_3. Therefore, we applied this method successively for total O_3 and total NO_2, obtaining the respective correlations with EDD_{90+}, while the other variable remained constant. To better understand and describe the results, classification criteria according to the type of correlation and the respective level of significance were established.

Additionally, having generated monthly EDD_{90+} thresholds, these results were grouped by year to estimate (a) the number of times (frequency) that a pixel is repeated under this condition each year, and (b) the number of days per year that registered this condition.

3. Results

3.1 Spatial and temporal distribution over Rio Grande do Sul State

The average daily ultraviolet erythemal irradiance for Rio Grande do Sul State, derived from OMI observations for the 15-year studied period, is presented in Figure 3a. Values vary from 3300 to 3700 J m^{-2}, with a steady irradiance gradient in latitude of about 66.7 J m^{-2} $degree^{-1}$, decreasing southwards. The long-term spatiotemporal variations are presented in Figure 3b, with values from 1.8 to 3.6%, a fluctuation

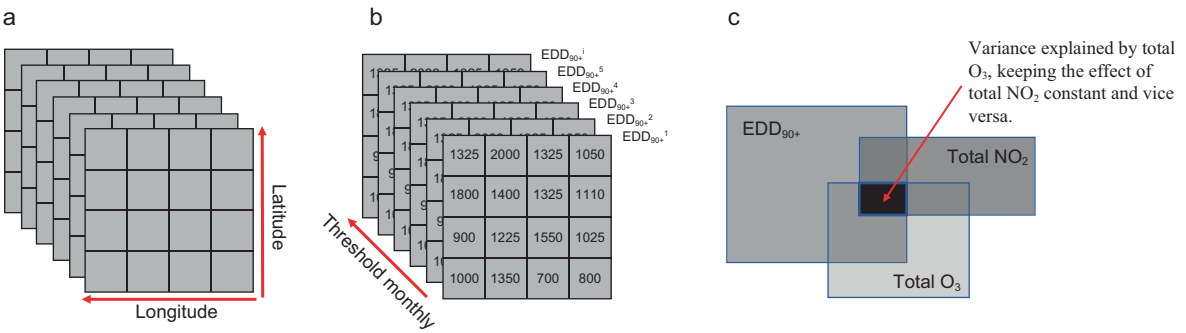

Fig. 2. Stages to evaluate the relationships with higher values of erythemal daily doses.

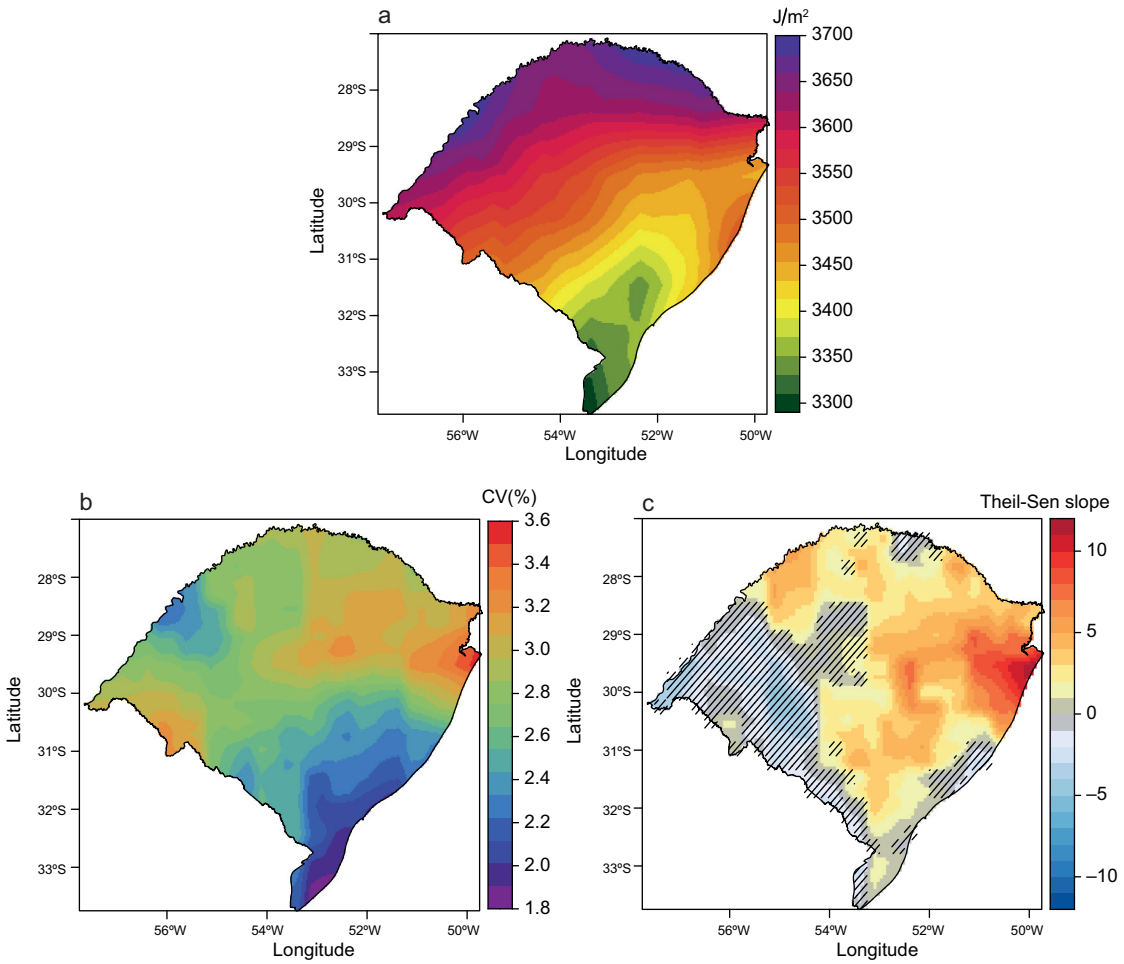

Fig. 3. Spatial distribution of (a) multi-year average erythemal daily dose from 2006 to 2020 (J m^{-2}); (b) coefficients of variations (CV%); (c) long-term trends (Theil-Sen's slope value). Significant trends ($\alpha \leq 0.05$) are shown as hatched areas, where trends to increase are displayed as red gradients and to decrease as blue gradients.

that approximately follows the gradient shown in Figure 3a. Figure 3c shows that 29.76% of the area had a long-term decreasing trend, while 6.19% had a long-term increasing trend; the remaining state's area didn't record significant (α>0.05) trends. The largest increasing trends coincide with north-east areas, which have the highest elevations.

Monthly averages had values as high as 6028 J m^{-2} in December and as low as 1123 J m^{-2} in June (Fig. 4 and Table I). Besides, it was observed that April and August were the months with the largest changes in ultraviolet erythemal irradiance, dropping from 2811 J m^{-2} in April to 1633 J m^{-2} in May and the inverse between August (1746 J m^{-2}) to September (2666 J m^{-2}) (Fig. 4, Table I). Regarding seasonal variations, these are more intense in the spring-summer period (4007 J m^{-2} to 5411 J m^{-2}) rather than in the autumn-winter period (1378 J m^{-2} to 2899 J m^{-2}) (Table I).

Considering that the ultraviolet erythemal irradiance in Rio Grande do Sul has a defined spatial and temporal pattern (Figs. 3, 4), and based on the 90th percentile for each pixel in each month (see Table SI in the supplementary material), we derived that the highest incidence of high values of ultraviolet erythemal irradiance took place in 2006 (a maximum of 67 occurrences per pixel and a total of 157 days), and the lowest incidence was recorded in 2011

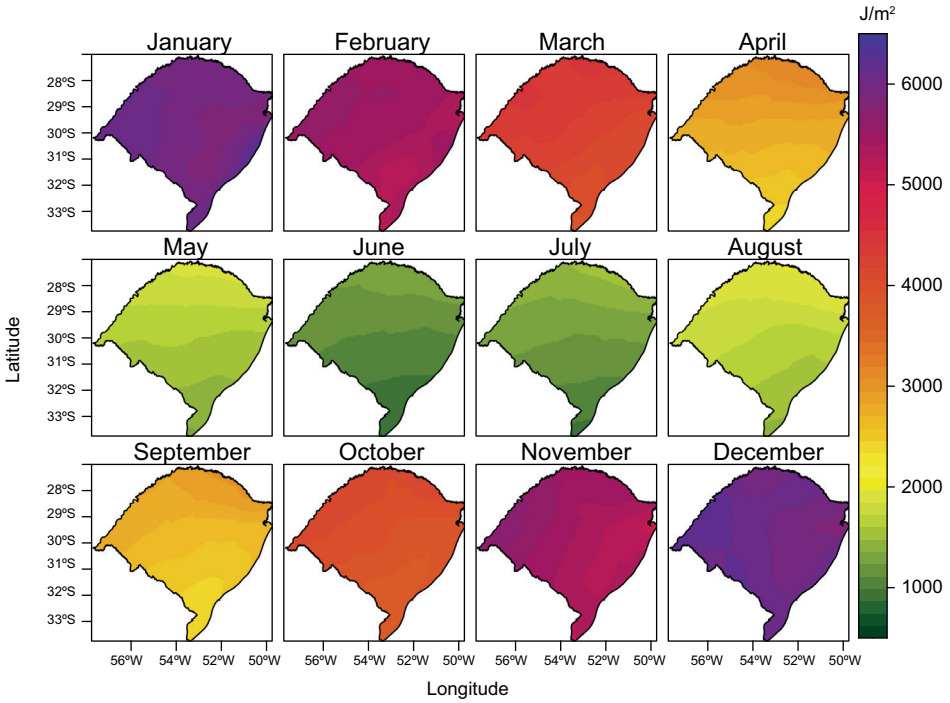

Fig. 4. Spatiotemporal distribution of monthly erythemal daily dose values (J m^{-2}) in Rio Grande do Sul from 2006 to 2020.

(a maximum of 20 occurrences per pixel and a total of 49 days) (Fig. 5).

The temporal relationships of total O_3 and total NO_2 with the higher values of ultraviolet erythemal irradiance are presented in Figure 6. It is observed that ultraviolet erythemal irradiance and total NO_2 present a similar pattern throughout the year with a minimum between the months that correspond to winter and maximum between the months that correspond to summer (Fig. 6a, c). Meanwhile, total O_3 exhibits minimum in summer and maximum in spring (Fig. 6b).

The partial ($r_{partial}$) pixel-to-pixel relationships between EDD_{90+} and total O_3 and total NO_2 vary by month (see Tables SII-SXIII in the supplementary material). In particular, we observed that occurrences of EDD_{90+} can be grouped in five situations (Table II), as follows: (a) pixels where there is a dominant negative correlation of EDD_{90+}, both with total O_3 and total NO_2; (b) pixels where there is a negative correlation with total O_3 and a positive one with total NO_2; (c) negative correlation predominates with total NO_2; (d) negative correlation predominates with total O_3, and (e) cases where EDD_{90+} occurrence is not explained by its correlation neither with total O_3 nor total NO_2.

The spatiotemporal distribution of these five situations is shown in Figure 7a, b, in terms of the percentages which explain the EDD_{90+} observations. From the analysis of results presented in Figure 7, it is suggested that total O_3 is the main factor explaining EDD_{90+} observations in all months, having a weight ranging from 25% (April) to 93% (November), with the notable exception of May, where its contribution (and of all other considered factors) is not significant. Synergies, either positive or negative, of total O_3 and NO_2 did not seem to play significant roles in EDD_{90+} observations, while total NO_2 explains EDD_{90+} observations at most for 4% of all pixels. On the other hand, between 5 to 96% of pixels with EDD_{90+} seem not to be linked neither to O_3 nor to NO_2, with higher frequencies in January (40% of the area) and May (96% of the area). EDD_{90+} data for these months remains mostly unexplained by our approach.

Table I. Historical erythemal daily dose (J m^{-2}) means in Rio Grande do Sul State, Brazil (2006-2020)*.

		2006	2007	2008	2009	2010	2011	2012	2013	2014	2015	2016	2017	2018	2019	2020	Average age
	Min	3268.80	3150.66	3147.99	3047.56	3062.55	2923.35	3144.24	3127.65	3062.54	3038.59	3107.56	3098.80	3103.57	3066.23	3258.64	3523.18
	Max	4048.69	3816.12	3890.14	3834.19	3938.40	3817.10	3948.04	3980.54	3766.24	3817.86	3938.17	3898.87	3950.04	3832.75	4047.60	
	Avg	3682.38	3448.17	3557.41	3455.17	3519.18	3423.95	3579.51	3592.31	3445.45	3388.14	3539.02	3526.36	3538.92	3478.90	3672.87	
	SD	169.21	140.71	155.85	167.83	191.46	180.91	164.58	186.94	152.03	169.42	178.87	168.47	185.78	155.05	181.05	
January	Min	5488.48	5939.72	5617.14	5504.68	4961.95	4994.64	6129.48	5905.89	5352.54	5365.28	5844.16	5643.63	5064.32	4578.50	5716.81	5961.76
	Max	6429.91	6797.85	6359.55	6183.63	6557.13	6215.91	6800.09	6674.06	6503.99	6242.56	6679.80	6385.24	6298.20	6154.74	6395.92	
	Avg	5894.54	6279.19	6080.60	5856.46	5843.93	5718.32	6452.78	6283.06	6005.87	5741.27	6237.72	5908.81	5681.96	5431.39	6010.57	
February	Min	5131.20	5251.41	4581.02	5082.78	4674.11	4193.23	4538.52	4412.04	4767.73	4971.58	4879.41	4871.09	5434.91	4965.13	5298.93	5430.43
	Max	5907.30	6044.07	5697.91	6044.57	6082.00	5348.34	6213.93	5603.45	5808.65	6007.45	5841.39	5684.70	6162.54	5623.77	5875.65	
	Avg	5608.42	5558.54	5372.52	5590.69	5531.27	5005.12	5423.73	5091.80	5335.45	5317.14	5479.22	5292.31	5883.53	5365.86	5600.85	
March	Min	3916.93	3546.14	3833.16	3834.76	4105.68	3793.35	3690.78	3638.05	3864.86	4158.70	3551.23	3636.17	3938.33	3722.94	4022.40	4252.25
	Max	4759.97	4738.58	4565.17	4866.91	4760.19	4438.87	4823.19	4177.45	4381.57	4527.89	4273.16	4464.31	4847.67	4322.19	5116.54	
	Avg	4410.86	4025.67	4255.23	4373.04	4456.69	4157.43	4495.57	3954.00	4129.94	4346.50	3868.19	4232.09	4390.95	4046.54	4641.13	
April	Min	2326.92	2455.26	2462.56	2552.55	2464.89	2279.12	2342.64	2412.18	2336.02	2585.23	1657.28	2164.06	2279.33	2382.82	2447.82	2811.85
	Max	3510.89	3172.53	3097.19	3580.86	3049.51	3114.04	3120.64	3500.83	3072.16	3155.04	3092.69	3185.53	3400.84	3191.08	3471.86	
	Avg	2975.73	2800.14	2846.04	3093.56	2685.01	2756.59	2762.93	2936.22	2719.92	2925.25	2336.12	2615.73	2918.77	2727.55	3078.20	
May	Min	1405.48	1261.47	1302.16	1417.23	1256.34	1287.07	1447.21	1319.54	1249.94	1356.93	1186.56	1256.72	1328.20	1337.50	1530.71	1633.16
	Max	2358.26	1764.32	2045.70	1937.72	1646.95	2037.09	2150.80	2002.00	1903.50	1931.15	1733.36	1687.89	2001.26	1627.08	2025.22	
	Avg	1804.05	1564.14	1717.16	1707.28	1417.34	1698.00	1857.55	1660.58	1547.57	1649.24	1530.44	1462.03	1583.99	1534.18	1763.86	
June	Min	913.73	804.79	885.78	824.74	865.82	879.28	826.25	975.40	791.18	940.61	782.16	998.74	852.47	802.04	857.91	1123.32
	Max	1479.06	1185.81	1289.37	1322.81	1427.01	1219.37	1328.42	1381.97	1177.11	1529.54	1357.12	1356.21	1223.61	1595.85	1286.04	
	Avg	1206.58	996.13	1099.70	1161.73	1094.31	1101.48	1074.86	1222.13	987.52	1182.22	1131.44	1153.66	1069.88	1287.23	1081.01	

*Data obtained from the OMI dataset.

Table I. Historical erythemal daily dose (J m^{-2}) means in Rio Grande do Sul State, Brazil (2006-2020)*.

		2006	2007	2008	2009	2010	2011	2012	2013	2014	2015	2016	2017	2018	2019	2020	Average age
July	Min	992.79	892.97	1073.82	1017.59	894.56	902.76	1064.08	1007.08	836.25	1002.54	892.31	928.12	743.58	933.30	996.78	1266.24
	Max	1724.80	1306.05	1868.98	1376.06	1493.15	1444.95	1391.53	1772.42	1420.21	1417.55	1682.35	1773.31	1521.86	1512.09	1556.63	
	Avg	1364.39	1139.92	1358.41	1254.90	1233.95	1122.99	1278.12	1425.48	1205.34	1159.73	1347.39	1495.27	1072.57	1215.55	1319.58	
August	Min	1393.45	1142.04	1570.57	1410.61	1446.86	1240.69	1380.80	1449.65	1611.09	1257.35	1467.05	1294.07	1396.50	1467.94	1519.99	1746.56
	Max	2025.51	1820.27	1919.62	1888.74	2029.95	1788.92	2154.31	1991.12	2177.76	2252.10	1976.43	2094.30	1932.47	2248.12	2216.56	
	Avg	1796.03	1448.47	1752.28	1615.48	1705.71	1564.51	1789.24	1715.55	1924.75	1793.68	1788.36	1829.37	1645.72	1861.23	1967.97	
September	Min	2666.08	2157.96	2172.60	2117.35	2226.36	2372.50	2319.42	2138.77	2369.27	2299.69	2441.69	2295.98	2178.74	2521.37	2228.43	2666.57
	Max	3089.37	3049.60	2924.10	2606.62	3162.04	3094.03	3078.70	3008.47	2747.02	3205.11	3392.04	3236.68	2814.52	3297.93	3217.45	
	Avg	2881.63	2528.25	2579.68	2398.34	2582.10	2633.46	2668.19	2647.56	2527.15	2729.82	2984.77	2694.28	2565.38	2947.72	2630.15	
October	Min	3932.25	3218.74	3429.20	3606.20	3916.43	3174.74	3424.19	3811.28	3553.57	3442.41	3638.36	3267.41	3352.05	3139.08	3586.36	3945.37
	Max	4534.77	3796.06	3944.03	4604.51	4756.87	4794.01	3964.24	4667.41	4425.30	4133.68	4664.19	4060.87	4321.33	4004.53	5037.91	
	Avg	4342.24	3401.74	3687.50	4130.93	4332.84	4083.44	3615.90	4249.34	4001.07	3783.76	4073.70	3640.47	3917.30	3595.26	4325.11	
November	Min	4811.50	5289.39	4943.70	3938.55	4630.76	4984.41	5322.94	4970.05	4824.56	4360.12	5352.40	5117.16	5193.20	4940.17	4884.87	5411.89
	Max	5904.39	5866.41	6287.10	5099.73	5817.45	5901.41	5989.90	6207.80	5637.73	5246.93	6067.33	6268.46	6094.22	5744.24	5839.23	
	Avg	5381.80	5573.39	5749.70	4365.35	5251.96	5473.05	5742.53	5486.37	5391.29	4770.12	5674.64	5852.64	5767.54	5361.81	5336.20	
December	Min	6246.74	5848.03	5904.21	5263.71	5306.82	4978.41	5244.60	5491.89	5193.51	4722.65	5598.16	5712.44	5481.18	6004.03	6012.68	6028.75
	Max	6860.07	6251.92	6682.90	6498.12	6478.56	6408.23	6360.69	6779.48	5939.91	6165.36	6498.18	6588.90	6782.01	6671.44	6532.23	
	Avg	6522.29	6062.50	6190.04	5914.31	6095.00	5772.99	5792.72	6435.61	5569.49	5258.93	6016.23	6139.60	5969.40	6372.44	6319.77	
Summer	Min	5622.14	5679.72	5367.46	5283.72	4980.96	4722.10	5304.20	5269.94	5104.59	5019.84	5440.58	5409.05	5326.80	5182.55	5676.14	5806.98
	Max	6399.09	6364.61	6246.79	6242.11	6372.56	5990.83	6458.24	6352.33	6084.18	6138.46	6339.79	6219.61	6414.25	6149.98	6267.93	
	Avg	6008.42	5966.74	5881.05	5787.15	5823.40	5498.81	5889.74	5936.82	5636.94	5439.11	5911.05	5780.24	5844.96	5723.23	5977.07	
	Min	2549.78	2420.96	2532.63	2601.51	2608.97	2453.18	2493.54	2456.59	2483.60	2700.29	2131.69	2352.32	2515.29	2481.09	2666.98	

*Data obtained from the OMI dataset.

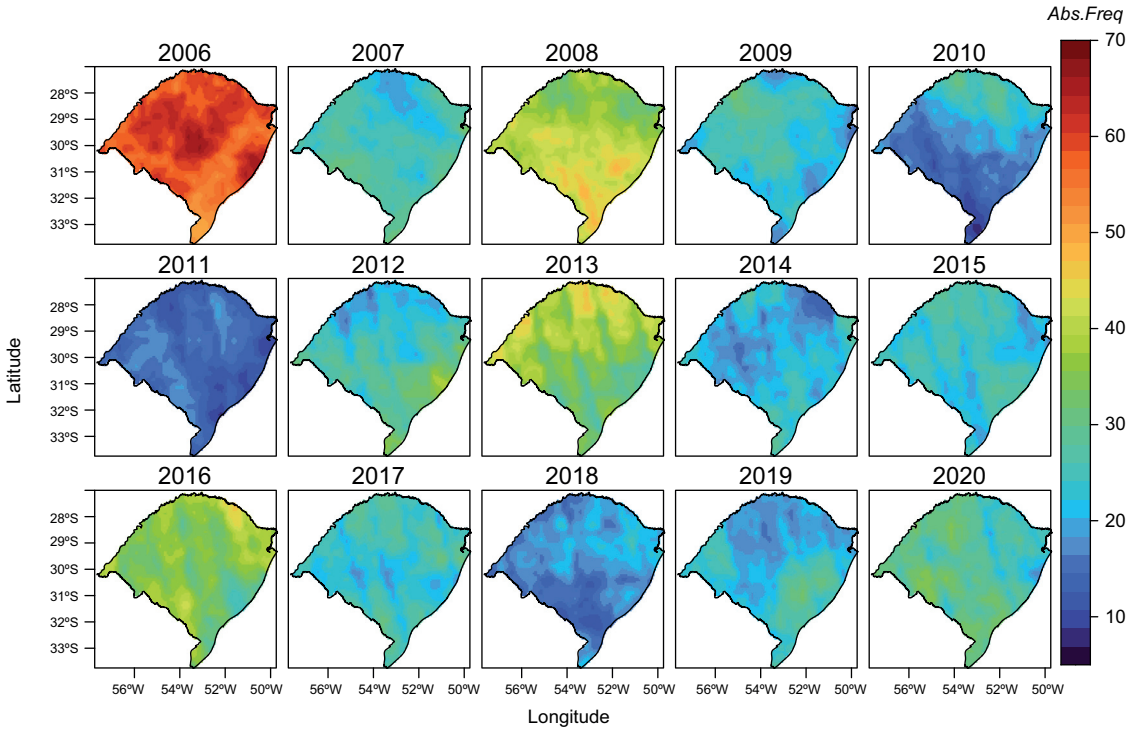

Fig. 5. Occurrence of spatiotemporal distribution of high erythemal daily dose values above the 90th percentile (EDD_{90+}).

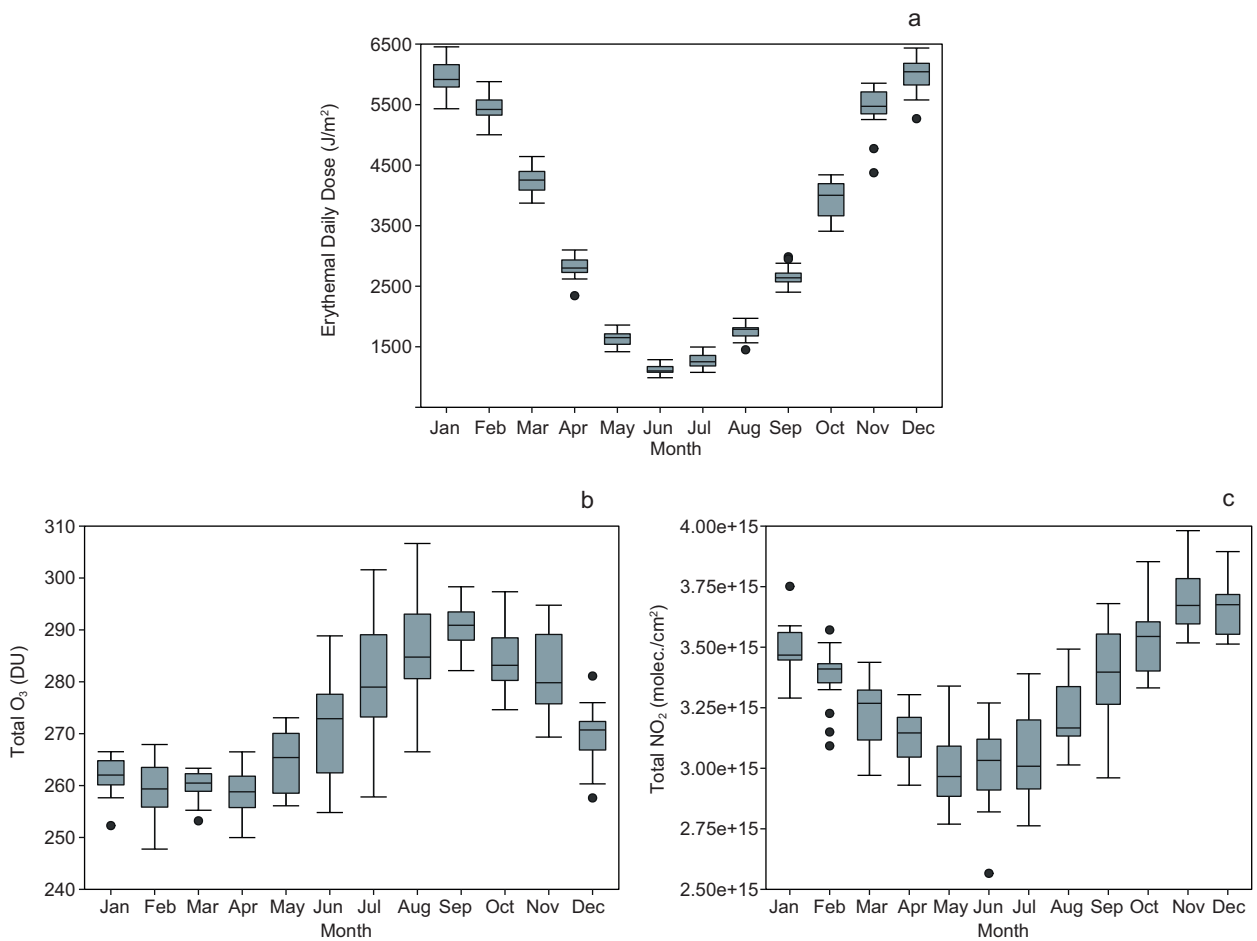

Fig. 6. Monthly mean of (a) erythemal daily dose, (b) total ozone, and (c) total nitrogen dioxide at Rio Grande do Sul for the period 2006-2020.

Table II. Classes according to partial correlation coefficients (r_{part}).

Clasification criteria	Class
rpartial[a] ≤ 0 & rpartial[b] ≤ 0; pvalue[a] ≤ 0.05 & pvalue[b] ≤ 0.05	TO_3–TNO_2
rpartial[a] ≥ 0 & rpartial[b] ≤ 0; pvalue[a] ≤ 0.05 & pvalue[b] ≤ 0.05	TO_3–TNO_2
rpartial[b] ≤ 0; pvalue[a] ≥ 0.05 & pvalue[b] ≤ 0.05	TO_3
rpartial[a] ≤ 0; pvalue[a] ≤ 0.05 & pvalue[b] ≥ 0.05	TNO_2
pvalue[a] ≥ 0.05 & pvalue[b] ≥ 0.05	Unexplained

[a]Total NO_2 (TNO_2); [b]total O_3 (TO_3).

4. Discussion

4.1 Spatial and temporal distribution over the Rio Grande do Sul State

The latitude dependence of ultraviolet erythemal irradiance within Rio Grande do Sul shown in Figure 3a is part of an ampler dependence already reported (Corrêa, 2015). Even if the overall ultraviolet irradiance in southern Brazil, and especially in Rio Grande do Sul, presents lower values if compared with northern regions, detailed knowledge of its magnitude and distribution is of interest by demographical reasons: the state presents the country's highest rates of melanoma cancer, a fact that is attributed to a higher percentage of people of Caucasian or European origin that present a greater predisposition to develop this pathology when exposed to UV radiation (Lee-Taylor et al., 2010; Corrêa, 2015; Imanichi et al., 2017; INCA, 2020). From Figure 3a it can be seen that UV erythemal irradiance varies significantly across the state, a perception that is reinforced by the results presented in Figure 3b and especially in Figure 3c, which suggest that irradiance had a positive time variation in a non-negligible fraction of the state's area during the studied period. Presently, information on skin cancer incidence in different regions of the state is still lacking, and this study provides useful information for the understanding of data that eventually will be available and the corresponding management. It is also important to note that the erythemal ultraviolet irradiance received in the fall of 2020 (with 3161 J m^{-2}) was higher than in the previous 14 autumns, in agreement with what was reported by Becerra-Rondón et al. (2021) on increases in the ultraviolet radiation index for that season in previous years. Additionally, we also note that the highest EDD values, which have been measured in 2006, coincide with a year of very low solar activity, as measured by the number of solar spots, while the lowest EDDs have been measured in 2011, that is, about a half solar cycle after 2006 (Rampelotto et al., 2009; Valachovic and Zurbenko, 2014; BOM, 2021).

Presently, we observe that the northeast part of the study area has the lowest latitudes and the highest altitudes, associated with the highest radiation values and with changes in intensity according to the period (for the monthly and seasonal case) (Fig. 4). This behavior is due, at least in part, to the fact that at higher sites the path through the atmosphere is shorter and scattering processes (Rayleigh and Mie) are not as important compared to lower sites, where radiation is reduced by increasing density and atmospheric components, which promotes greater attenuation (Ziemke et al., 2000). This effect is intensified when combined with the variation of the solar zenith angles (geographical and astronomical effects) (Schmucki and Philipona, 2002). Although these two effects establish a spatial and temporal distribution pattern in our study area, changes in cloud cover, temperature, secondary effects of the Antarctic ozone hole, and other variables (e.g., ozone, aerosols, and air pollutants) also greatly influence short- and long-term variations (Kirchhoff et al., 1996; Koronakis et al., 2002; Schmucki and Philipona, 2002; Guarnieri et al., 2004; Kerr and Fioletov, 2008; Salgado et al., 2010; Schmalfuss et al., 2014; Nunes et al., 2020).

4.2. Relationships of total O_3 and total NO_2 with high values of erythemal daily dose

Even if the temporal behavior of total O_3 and total NO_2 (which affect ultraviolet radiation [Fig. 6b, c]) is well defined, the simultaneous presence of more than one of them can lead to non-linear interactions involving complex absorption and scattering processes (Kirchhoff et al., 2000; Krotkov et al., 2001;

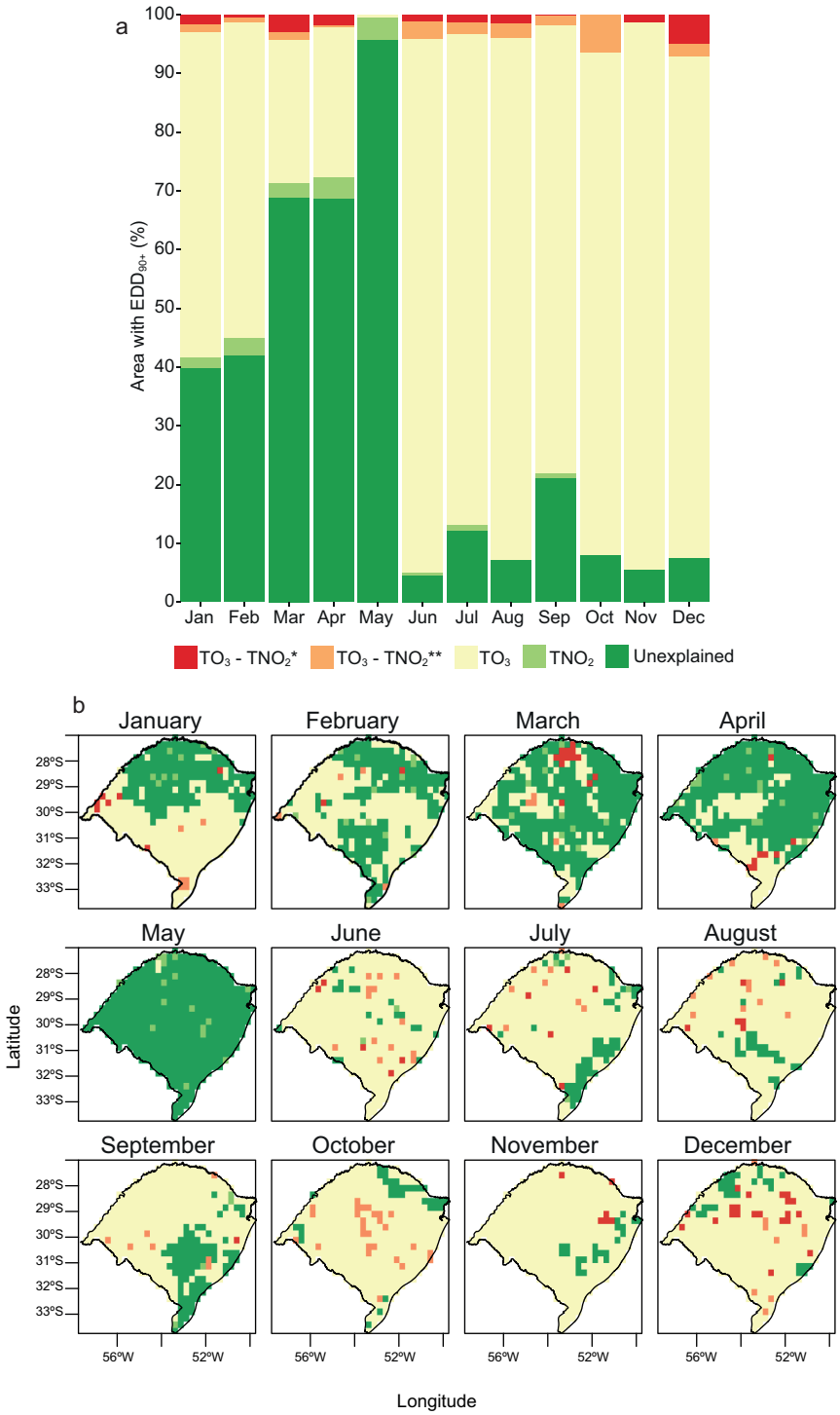

Fig. 7. Factors affecting the spatiotemporal variability of EDD_{90+} in Rio Grande do Sul: (a) monthly percentage of area explained by total O_3 or total NO_2, and their combinations; (b) its spatial location.

Koronakis et al., 2002). Moreover, the magnitude of the ultraviolet intensity varies in function of the chosen period (daily, monthly, and annual mean), and from geographical characteristics (Kerr, 2005; Ialongo et al. 2011; Čížková et al., 2018). From these perceptions and considering the atmospheric processes and associated health hazards characteristic of our study area, we highlighted where higher values of ultraviolet radiation occurred, spatially and temporally (EDD_{90+}) (Fig. 5). From these results, the relationships of the two modulating factors (total O_3 and total NO_2) with respect to EDD_{90+} were investigated.

We found that for nine months of an average year (from June to February) between 53 to 93% of the study area have EDD_{90+} primarily associated with total O_3 in the form of a negative correlation (Fig. 7a, b). This behavior has also been reported in other works under all weather conditions (Kerr and McElroy, 1993; Fioletov et al., 1997; Guarnieri et al. 2004; Rieder et al., 2010; Bernhard et a., 2013; Lopo et al., 2014; Čížková et al., 2018; Raptis et al., 2021). In the remaining months (March to May) from 70 to 96% of the area have EDD_{90+} unexplained by total O_3 and/or total NO_2, being therefore attributed to variables not considered in this study. A large inversion of the total O_3 weight between May and June was observed. While it is true that total O_3 is the main driver of long-term variations in ultraviolet radiation intensities, it can also be argued that the solar zenith angle (SZA) and cloud cover are non-negligible factors in the short term, gaining more importance during autumn and summer, respectively (Lopo et al., 2014; de Bock et al., 2014; Čížková et al., 2018). In this context and considering the complexity of interactions with ultraviolet radiation, during autumn and winter Rio Grande do Sul State is also under the effect of atmospheric circulation patterns (equatorial Atlantic mass, tropical Atlantic, continental tropical, and polar) that promote the transport of flows of ozone-poor air from the tropics towards high latitudes, accompanied by higher air pressures that lead to clear or partially cloudy skies, leading to the incidences of EDD_{90+} (Stick et al., 2006; Rossato, 2011).

Meanwhile, although in a smaller proportion of the studied area (between 0.2-6.4%) throughout the year, the relationship of total NO_2 with EDD_{90+} values exists in three situations (Table II), depending of the pixels (regions) considered, which shows how the complexity of the interaction of more than one variable in time and space generates the same effect.

Associating our results and their derived perceptions to what has been reported elsewhere (Rieder et al., 2010; Cížková et al., 2018), high values of ultraviolet radiation tend to be associated to low total O_3 levels and with the absence of clouds or with partly cloudy skies. Furthermore, the influence of air pollutants (e.g., NO_2) over ultraviolet radiation is significant, acting in complex ways, even on cloudy days when the prevailing effect of clouds was expected. It was reported that two of these outcomes are that both high and low concentrations of NO_2 lead to higher ultraviolet radiation (Dickerson et al., 1997; WMO, 2020; Musiolková et al., 2021), which strongly suggests that although there are specific patterns for each variable depending on the season and cloud cover, the latter is possibly the most important, since it plays a crucial role in the influence of incident solar radiation during the day (Krotkov et al., 2001; Alados-Arboledas et al., 2003; Musiolková et al., 2021)

5. Conclusions

Human exposure to solar ultraviolet radiation has important public health implications, and evidences of hazards associated with UV overexposure have been reported in many investigations. Starting from these perceptions and taking them as motivation, this study used remote sensing data to analyze the spatiotemporal characteristics of EDDs in Rio Grande do Sul, a region where this important information is still lacking. Our results showed that (1) the annual average of the daily accumulated EDDs was 3523.18 J m^{-2}, with a long-term decreasing trend in 29.76% of the state's area; (2) places located in lower latitudes and higher altitudes had higher incidences of EDD; (3) there is a well-defined temporal pattern, with a higher average value in summer (5806.98 J m^{-2}) and a lower average value in winter (1378.71 J m^{-2}); (4) during the 15 years of the study (2006-2020), the highest number of days with high EDD was in 2006, a year of lower solar activity, and (5) the incidence of EDD_{90+} (the more intense radiation for the whole studied period) showed a negative correlation with total O_3, and in a few cases either positive or negative correlations

with total NO_2, however, the lack of correlations of EDD_{90+} with both total O_3 and total NO_2 in many instances (places and dates) is an indication that there are variables not considered in this study. Even if part of our generated EDD_{90+} data remains unexplained, our results on the spatiotemporal distribution of the highest incidence of this radiation can be relevant for official policies concerning the regional prevention of skin neoplasms, which are already among the highest in Brazil.

Acknowledgments

ABR acknowledges the Brazilian Agency Coordenação de Aperfeiçoamento de Pessoal de Nível Superior (CAPES) for her doctoral fellowship.

References

André IRN, Ferreira NJ, Conforte JC. 2003. Análise do comportamento do ozônio estratosférico na América do Sul e vizinhanças utilizando-se imagens do satélite NIMBUS7/TOMS. In: Proceedings of the 11th Brazilian Symposium on Remote Sensing, Belo Horizonte, 1117-1124.

Alados-Arboledas L, Alados I, Foyo-Moreno I, Olmo FJ, Alcántara, A. 2003. The influence of clouds on surface UV erythemal irradiance. Atmospheric Research 66: 273-290. https://doi.org/10.1016/S0169-8095(03)00027-9

Andrade R, Tiba C. 2016. Extreme global solar irradiance due to cloud enhancement in northeastern Brazil. Renewable Energy 86: 1433-1441. https://doi.org/10.1016/j.renene.2015.09.012

Antón M, Piedehierro AA, Alados-Arboledas L, Wolfran E, Olmo FJ. 2012. Extreme ultraviolet index due to broken clouds at a midlatitude site, Granada (southeastern Spain). Atmospheric Research 118: 10-14. https://doi.org/10.1016/j.atmosres.2012.06.007

Bais AF, Lubin D, Arola A, Bernhard G, Blumthaler M, Chubarova N, Erlick C, Gies HP, Krotkov NA, Lantz K, Mayer B, Mckenzie RL, Piacentini RD, Seckmeyer G, Slusser JR, Zerefos CS. 2007. Surface ultraviolet radiation: Past, present, and future. Chapter 7. In: Scientific assessment of ozone depletion: 2006 (Ennis CA, Ed.). Global Ozone Research and Monitoring Project. Report No. 50. World Meteorological Organization, Geneva, 58 pp

Bais AF, Mckenzie RL, Bernhard G, Aucamp PJ, llysa M, Madronich S, Tourpali K. 2015. Ozone depletion and climate change: Impacts on UV radiation. Photochemical and Photobiological Sciences 14: 19-52. https://doi.org/10.1039/C4PP90032D

Barnard WF, Wenny BN. 2010. Ultraviolet radiation and its interaction with air pollution. In: UV Radiation in global climate change (Gao W, Slusser JR, Schmoldt DL, Eds.). Springer, Berlin, 290-330. https://doi.org/10.1007/978-3-642-03313-1_11

Becerra-Rondón A, Ducati J, Haag R. 2021. Partial COVID-19 lockdown effect in atmospheric pollutants and indirect impact in UV radiation in Rio Grande do Sul, Brazil. Atmósfera 36: 143-154. https://doi.org/10.20937/ATM.53027

Bernhard G, Dahlback A, Fioletov V, Heikkilä A, Johnsen B, Koskela T, Lakkala K, Svendby T. 2013. High levels of ultraviolet radiation observed by ground-based instruments below the 2011 Arctic ozone hole. Atmospheric Chemistry and Physics 13: 10573-10590. https://doi.org/10.5194/acp-13-10573-2013

Bilbao J, Román R, de Miguel A, Mateos D. 2011. Long-term solar erythemal UV irradiance data reconstruction in Spain using a semiempirical method. Journal of Geophysical Research-Atmospheres 116, D22211. https://doi.org/10.1029/2011JD015836

BOM. 2021. The Sun and solar activity. Bureau of Meteorology. Space Weather Services. Available at: https://www.sws.bom.gov.au/Educational/2/3/6 (accessed on December 21, 2021).

Cardoso V. 2011. Efeitos da radiação ultravioleta-A e ultravioleta-B sobre os embriões do camarão de água-doce *Macrobrachium olfersii* (Crustacea, Decapoda) e o papel da radiação ultravioleta-A na fotorreativação. M.Sc. thesis. Federal University of Santa Catarina, Florianópolis, Brazil.

Caldwell M, Ballaré C, Bornman J, Flint S, Björn L, Teramura A, Kulandaivelu G, Tevini M. 2003. Terrestrial ecosystems, increased solar ultraviolet radiation and interactions with other climatic change factors. Photochemical and Photobiological Sciences 2: 29-38. https://doi.org/10.1039/B211159B

Corrêa M, Pires L. 2013. Doses of erythemal ultraviolet radiation observed in Brazil. International Journal of Dermatology 52: 966-973. https://doi.org/10.1111/j.1365-4632.2012.05834.x

Corrêa M. 2015. Solar ultraviolet radiation: Properties, characteristics and amounts observed in Brazil and

South America. Anais Brasileiros de Dermatologia 90: 297-313. https://doi.org/10.1590/abd1806-4841.20154089

Čížková K, Láska K, Metelka L, Staněk M. 2018. Reconstruction and analysis of erythemal UV radiation time series from Hradec Králové (Czech Republic) over the past 50 years. Atmospheric Chemistry and Physics 18: 1805-1818. https://doi.org/10.5194/acp-18-1805-2018

Davis A, Sims D. 1983. Weathering of polymers. Applied Science Publishers, England. https://doi.org/10.1002/pol.1984.130220709

De Bock V, de Backer H, van Malderen R, Mangold A, Delcloo A. 2014. Relations between erythemal UV dose, global solar radiation, total ozone column and aerosol optical depth at Uccle, Belgium. Atmospheric Chemistry and Physics 14: 12251-12270. https://doi.org/10.5194/acp-14-12251-2014.

Dickerson RR, Kondragunta S, Stenchikov G, Civerolo KL, Doddridge BG, Holben B. N. 1997. The impact of aerosols on solar ultraviolet radiation and photochemical smog. Science 278: 827-830. https://doi.org/10.1126/science.278.5339.827

Díaz S, Camilión C, Deferrari G, Fuenzalida H, Armstrong R, Booth C Paladini A, Cabrera S, Casiccia C, Lovengreen C, Pedroni J, Rosales A, Zagarese H, Vernet M. 2006. Ozone and UV radiation over southern South America: Climatology and anomalies. Photochemistry and Photobiology 82: 0031-8655. https://doi.org/10.1562/2005-09-26-RA-697

Efstathiou MN, Feretis H, Tzanis C, Christodoulakis J. 2005. Observed association between air pollution and the biologically effective solar ultraviolet irradiance. International Journal of Remote Sensing 26: 3487-3495. https://doi.org/10.1080/01431160500076566

Elsner JB, Jagger TH, Hodges RE. 2010. Daily tropical cyclone intensity response to solar ultraviolet radiation. Geophysical Research Letters 37: L09701. https://doi.org/10.1029/2010GL043091

Fahey DW, Hegglin MI, eds. 2011. Twenty questions and answers about the ozone layer: 2010 update. In: Scientific assessment of ozone depletion: 2010 (Ennis CA, Ed.). Global Ozone Research and Monitoring Project. Report No. 52. World Meteorological Organization, Geneva, 72 pp

Farman JC, Gardiner BG, Shanklin JD. 1985. Large losses of total ozone in Antarctica reveal seasonal ClO_x/NO_x interaction. Nature 315: 207-210. https://doi.org/10.1038/315207a0

Fioletov VE, Kerr JB, Wardle DI. 1997. The relationship between total ozone and spectral UV irradiance and its use for deriving total ozone from UV measurements. Geophysical Research Letters 24: 2997-3000. https://doi.org/10.1029/97GL53153

Fountoulakis I, Diémoz H, Siani AM, Laschewski G, Filippa G, Arola A, Bais AF, de Backer H, Lakkala K, Webb AR, de Bock V, Karppinen T, Garane K, Kapsomenakis J, Koukouli ME, Zerefos CS. 2020. Solar UV irradiance in a changing climate: Trends in Europe and the significance of spectral monitoring in Italy. Environments 7: 1. https://doi.org/10.3390/environments7010001

Gholamnia R, Abtahi M, Dobaradaran S, Koolivand A, Jorfi S, Khaloo S, Bagheri A, Hossein Vaziri M, Atabaki J, Alhouei F,Saeedi, R. 2021. Spatiotemporal analysis of solar ultraviolet radiation based on Ozone Monitoring Instrument dataset in Iran, 2005-2019. Environmental Pollution 287: 117643. https://doi.org/10.1016/j.envpol.2021.117643

Grant RH, Heisler GM. 2000. Estimation of ultraviolet-B irradiance under variable cloud conditions. Journal of Applied Meteorology 39: 904-916. https://doi.org/10.1175/1520-0450(2000)039<0904:EOUBIU>2.0.CO;2

Guarnieri RA, Guarnieri FL, Contreira DB, Padilha LF, Echer E, Pinheiro DK, Schuch AMP, Makita K, Schuch NJ. 2004. Ozone and UVB radiation anticorrelations at fixed solar zenith solar angles in southern Brazil. Geofísica Internacional 43: 17-22. https://doi.org/10.22201/igeof.00167169p.2004.43.1.209

Herman J. 2010. Changes in ultraviolet and visible solar irradiance, 1979 to 2008. In: UV radiation in global climate change (Gao W, Slusser JR, Schmoldt D., Eds.). Springer, Berlin, Heidelberg. https://doi.org/10.1007/978-3-642-03313-1_5

Huffman RE. 1992. Atmospheric ultraviolet remote sensing. Academic Press, California.

Ialongo I, Casale GR, Siani A.M. 2008. Comparison of total ozone and erythemal UV data from OMI with ground-based measurements at Rome station. Atmospheric Chemistry and Physics 8: 3283-3289. https://doi.org/10.5194/acp-8-3283-2008

Ialongo I, Arola A, Kujanpää J, Tamminen J. 2011. Use of satellite erythemal UV products in analysing the global UV changes. Atmospheric Chemistry and Physics 11: 9649-9658. https://doi.org/10.5194/acp-11-9649-2011

Iqbal M. 1983. An introduction to solar radiation. Academic Press, Toronto, New York, London.

Imanichi D, Moraes CF, Soteroi RDC, Gomes LO. 2017. Fatores de risco do câncer de pele não melanoma em idosos no Brasil. Available at: https://docs.bvsalud.org/biblioref/2017/03/832424/rdt_v22n1_3-7.pdf (accessed on November 18, 2021).

INCA. 2020. The cancer incidence in Brazil. National Institute of Cancer José Alencar Gomes (INCA). Available at: https://www.inca.gov.br/sites/ufu.sti.inca.local/files//media/document//estimativa-2020-incidencia-de-cancer-no-brasil.pdf (accessed on August 10, 2021).

Jebar MAA, Parisi AV, Downs NJ, Turner J .2019. Influence of clouds on OMI satellite total daily UVA exposure over a 12-year period at a southern hemisphere site. International Journal of Remote Sensing 41: 272-283. https://doi.org/10.1080/01431161.2019.1641243

Kendall MG. 1975. Rank correlation techniques. 4th ed. Charles Griffin, London.

Kerr JB, Mcelroy CT. 1993. Evidence for large upward trends of ultraviolet- B radiation linked to ozone depletion. Science 262: 1032-1034. https://doi.org/10.1126/science.262.5136.1032

Kerr JB. 2005. Understanding the factors that affect surface ultraviolet radiation. Optical Engineering 44: 041002. https://doi.org/10.1117/1.1886817.

Kerr JB, Fioletov VE. 2008. Surface ultraviolet radiation. Atmospheric Ocean 46: 159-184. https://doi.org/10.3137/ao.460108

Kirchhoff VWJH, Schuch NJ, Pinheiro DK, Harris JM. 1996. Evidence for an ozone hole perturbation at 30º south. Atmospheric Environment 30: 1481-1484, 1487-1488. https://doi.org/10.1016/1352-2310(95)00362-2

Kirchhoff VWJH, Echer E, Leme NP, Silva AA. 2000. A variação sazonal da radiação ultravioleta solar biologicamente ativa. Revista Brasileira de Geofísica 18: 63-74. https://doi.org/10.1590/S0102-261X2000000100006

Koronakis PS, Sfantosa GK, Paliatsosb AG, JKaldellisc K, Garofalakisd JE, Koronakie IP. 2002. Interrelations of UV-global/global/diffuse solar irradiance components and UV-global attenuation on air pollution episode days in Athens, Greece. Atmospheric Environment 36: 3173-3181. https://doi.org/10.1016/S1352-2310(02)00233-9

Koller LR. 1965. Ultraviolet radiation. John Wiley and Sons, New York.

Krotkov NA, Herman JR, Bhartia PK, Fioletov V, Ahmad Z. 2001. Satellite estimation of spectral UV irradiance. Effects of homogeneous clouds and snow. Journal of Geophysical Research 106: 11743-11759. https://doi.org/10.1029/2000JD900721

Krotkov NA, Carn SA, Krueger AJ, Bhartia PK, Yang K. 2006. Band residual difference algorithm for retrieval of SO_2 from the Aura Ozone Monitoring Instrument (OMI). IEEE Transactions on Geoscience and Remote Sensing 44: 1259-1266. https://doi.org/10.1109/TGRS.2005.861932

Levelt PF, van den Oord GHJ, Dobber MR, Mälkki A, Visser H, de Vries J, Stammes P, Lundell JOV, Saari H. 2006. The Ozone Monitoring Instrument. IEEE Transactions on Geoscience and Remote Sensing 44: 1093-1101. https://doi.org/10.1109/TGRS.2006.872333

Lee-Taylor J, Madronich S, Fischer C, Mayer B. 2010. A climatology of UV radiation, 1979-2000: 65S-65N. In: UV radiation in global climate change (Gao W, Slusser JR, Schmoldt DL, Eds.). Springer, Berlin, Heidelberg. https://doi.org/10.1007/978-3-642-03313-1_1

Liu H, Hu B, Zhang L, Zhao XJ, Shang KZ, Wang YS, Wang J. 2017. Ultraviolet radiation over China: Spatial distribution and trends. Renewable and Sustainable Energy Reviews 76: 1371-1383. https://doi.org/10.1016/j.rser.2017.03.102

Livi FP. 2002. O clima em Porto Alegre no século XX: uma análise de séries temporais. M.Sc. thesis. Federal University of Rio Grande do Sul, Porto Alegre, Brazil.

Lopo AB, Spyrides MHC, Lucio PS, da Silva SMP. 2014. UV extreme events in northeast of Brazil. Ciência e Natura 36: 482-490. https://doi.org/10.5902/2179460X12816

Mann HB. 1945. Nonparametric tests against trend. Econometrica 13: 245-259. https://doi.org/10.2307/1907187

Meleti C, Bais AF, Kazadzis S, Kouremeti N, Garane K, Zerefos C. 2009. Factors affecting solar ultraviolet irradiance measured since 1990 at Thessaloniki, Greece. International Journal of Remote Sensing 30: 4167-4179, https://doi.org/10.1080/01431160902822864

Musiolková M, Huszár P, Navrátil M, Špunda V. 2021. Impact of season, cloud cover, and air pollution on different spectral regions of ultraviolet and visible incident solar radiation at the surface. Quarterly Journal of the Royal Meteorological Society 147: 2834-2849. https://doi.org/10.1002/qj.4102

McKinlay AF, Diffey BL. 1987. A reference action spectrum for ultraviolet induced erythemal in human skin. In: Human exposure to ultraviolet radiation: Risks and regulations (Passchler WF, Bosnjakovic BFM, Eds.). Elsevier, Amsterdam, 83-87.

NASA. 2021. Earth Observatory. National Aeronautics and Space Administration. Available at: https://urs.earthdata.nasa.gov (accessed on September 1, 2021).

Nunes MD, Mariano GL, Alonso MF. 2020. Variabilidade espaço-temporal da coluna total de ozônio e sua relação com a radiação ultravioleta na América do Sul. Revista Brasileira de Geografia Física 13: 2053-2073.

R Core Team. 2021. R: A language and environment for statistical computing. R Foundation for Statistical Computing, Vienna, Austria. Available at: https://www.R-project.org/ (accessed on September 15, 2021).

Rampelotto PH, da Rosa MB, Schuch NJ. 2009. Solar cycle and UV-B comparison for South America – South of Brazil (29º S, 53º W). In AIP Conference Proceedings. American Institute of Physics 1100: 490-493. https://doi.org/10.1063/1.3117028

Raptis IP, Eleftheratos K, Kazadzis S, Kosmopoulos P. 2021. The effect of ozone and aerosols on erythemal irradiance in a low ozone event. Atmosphere 12: 145. https://doi.org/10.3390/atmos12020145

Rieder HE, Staehelin J, Weihs P, Vuilleumier L, Maeder JA, Holawe F, Blumthalere M, Lindfors A, Peter T, Simic S, Spichtinger P, Wagner JW, Walker D, Ribatet M. 2010. Relationship between high daily erythemal UV doses, total ozone, surface albedo and cloudiness: An analysis of 30 years of data from Switzerland and Austria. Atmospheric Research 98: 9-20. https://doi.org/10.1016/j.atmosres.2010.03.006.

Robinson N. 1966. Solar radiation. Elsevier, Amsterdam.

Rodríguez JC. 2017. Características da radiação ultravioleta solar e seus efeitos na saúde humana nas cidades de La Paz – Bolívia e Natal – Brasil. Ph.D. thesis. Federal University of Rio Grande do Norte, Natal, Brazil.

Rossato MS. 2011. Os climas do Rio Grande do Sul: variabilidade, tendências e tipologia. Ph.D. thesis. Graduate Program in Geography. Institute of Geosciences, Universidad Federal de Rio Grande do Sul, Porto Alegre, Brazil. Available at: http://hdl.handle.net/10183/32620 (accessed on June 1, 2021).

Salgado CAC, Paes Leme NM, Zamorano F, Quel EJ, Viana R. 2010. Influence of the ozone hole on the American. South Cone 1992-2009. In: Proceedings of the Meeting of the Americas, Foz do Iguaçu, Brazil.

Seinfeld JH, Pandis SN. 1998. Atmospheric chemistry and physics: From air pollution to climate change. Wiley Interscience, New York.

Silva F, Oliveira H, Marinho G. 2008. Variação do índice de radiação solar ultravioleta em Natal-RN entre 2001 e 2007. In: Brazilian Solar Energy Congress and III ISES Latin American Regional Conference, Florianópolis, Brazil.

Schmalfuss LSM, Mariano GL, Pinheiro DK, Peres LV. 2014. Análise dos dois principais fatores de decaimento da coluna total de ozônio sobre o sul da América do Sul. Ciência e Natura 36: 415-422. https://doi.org/10.5902/2179460X12812

Schmucki DA, Philipona R. 2002. UV radiation in the Alps: The altitude effect. Proceedings of SPIE 4482: 234-239. https://doi.org/10.1117/12.452923

Sliney DH. 2007. Radiometric quantities and units used in photobiology and photochemistry: Recommendations of the Commission Internationale de l'Eclairage. Photochemistry and Photobiology 83: 425-432. https://doi.org/10.1562/2006-11-14-RA-1081

Stick C, Krüger K, Schade NH, Sandmann H, Macke A. 2006. Episode of unusual high solar ultraviolet radiation over central Europe due to dynamical reduced total ozone in May 2005. Atmospheric Chemistry and Physics 6: 1771-1776. https://doi.org/10.5194/acp- 6-1771-2006.

Tanskanen A, Krotkov NA, Herman JR, Arola A. 2006. Surface ultraviolet irradiance from OMI. IEEE Transactions on Geoscience and Remote Sensing 44: 1267-1271. https://doi.org/10.1109/TGRS.2005.862203

Tiegte JE, Diamond SA, Ankley GT, DeFoe DL, Holcombe GW, Jensen KM, Degitz SJ, Elonen GH, Hammer E. 2007. Ambient solar UV radiation causes mortality in larvae of three species of rana under controlled exposure conditions. Photochemistry and Photobiology 74: 261-268. https://doi.org/10.1562/0031-8655(2001)0740261ASURCM2.0.CO2

Valachovic E, Zurbenko I. 2014. Skin cancer, irradiation, and sunspots: The solar cycle effect. BioMed Research International, 538574. https://doi.org/10.1155/2014/538574

Wakamatsu S, Uno I, Veda H, Uehara K, Tateishh H. 1989. Observational study of stratospheric ozone intrusions into the lower troposphere. Atmospheric Environment 23: 1815-1826. https://doi.org/10.1016/0004-6981(89)90065-6

Wolfram EA, Salvador J, Orte F, Bulnes D, D'Elia R, Antón M, Alados-Arboledas L, Quel E. 2013. Study of cloud enhanced surface UV radiation at the atmospheric observatory of Southern Patagonia, Río Gallegos, Argentina. In AIP Conference Proceedings 1531: 907. https://doi.org/10.1063/1.4804918

WMO. 2007. Scientific assessment of ozone depletion: 2006. Global Ozone, Research and Monitoring Project. Report No. 50. World Meteorological Organization, Geneva, Switzerland.

WMO. 2020. Arctic ozone depletion reached record level. World Meteorological Organization. Available at: https://public.wmo.int/en/media/news/arctic-ozone-depletion-reached-record-level (accessed on August 10, 2020).

Zaratti F, Piacentini RD, Guillén HA, Cabrera SH, Liley JB, McKenzie RL. 2014. Proposal for a modification of the UVI risk scale. Photochemical & Photobiological Sciences 13: 980-985. https://doi.org/10.1039/C4PP00006D

Ziemke JR, Chandra S, Herman J, Varotsos C. 2000. Erythemal weighted ultraviolet trends over northern latitudes. Radiation Protection Dosimetry 91: 157-160. https://doi.org/10.1093/oxfordjournals.rpd.a033188